

# HCN Infrared Chemiluminescence from the H + ICN Reaction

E. Arunan and D. W. Setser\*

Department of Chemistry, Kansas State University, Manhattan, Kansas 66506 (Received: March 12, 1991)

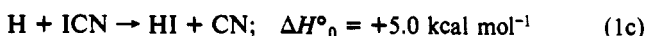
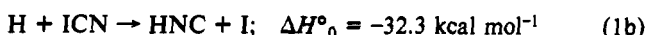
The title reaction has been studied in a flowing afterglow reactor at 0.5 Torr of Ar using infrared chemiluminescence. The HCN ( $\nu_1$ ,  $\nu_2$ ,  $\nu_3$ ) vibrational distribution was determined by simulating the observed emission spectrum using known vibrational-rotational constants. Due to the strong overlap between several bands, it was possible to fit the experimental spectrum with different combinations of bending and CH stretch quanta. But, the  $\langle f_v \rangle$  for the different distributions was always about 0.6. The favored distribution in  $\nu_3$  is inverted extending to  $\nu_3 = 4$ , with several quanta in the bending mode. The total HCN emission intensity observed from H + ICN reaction was compared with that of HCl from H + Cl<sub>2</sub> reaction under identical conditions, and a 300 K rate constant for HCN formation of  $(2.0 \pm 0.4) \times 10^{-12} \text{ cm}^2 \text{ s}^{-1}$  was assigned. Weak emission from  $\nu_3$  of HNC was also observed, probably arising from a minor channel leading to HNC + I.

## Introduction

Infrared chemiluminescence (IRCL) is one of the techniques that has led to our detailed understanding of molecular reaction dynamics for reactions giving HX (X = F, Cl, Br, O) as a product.<sup>1</sup> However, this technique has not been widely applied to reactions yielding polyatomic products for several reasons.<sup>2</sup> Einstein coefficients for infrared emission are relatively small and not well established. Furthermore, the emission spectroscopy of highly excited levels of polyatomic molecules becomes complicated since more than one vibrational mode can be excited during the reaction. Finally, intramolecular and intermolecular vibrational relaxation may become important, making the determination of nascent product distributions difficult.

In the extension of IRCL to polyatomic molecules, hydrogen cyanide appears to be an excellent candidate. Einstein coefficients for  $\Delta\nu_3 = 1$  emission are large, nearly double that of HCl. (We use the notation  $\nu_1$  (2127 cm<sup>-1</sup>) for CN stretch,  $\nu_2$  (727 cm<sup>-1</sup>) for bending and  $\nu_3$  (3442 cm<sup>-1</sup>) for CH stretch). The C-H bond is highly anharmonic and  $\Delta\nu_3 = 1$  emission from higher vibrational levels are well resolved. Excitation in the bending mode and CN stretch also shift the  $\Delta\nu_3 = 1$  emission spectrum such that the complete distribution can be assigned. In fact, Marciq et al.<sup>3</sup> used IRCL from HCN to estimate the vibrational distribution from H-abstraction reactions of cyanide ion. However, they used band-pass filters to collect the emission, and the vibrational distributions were hard to assign. We report here the results from IRCL studies of the H + ICN reaction using an FTIR spectrometer to record the HCN  $\Delta\nu_3 = 1$  emission.

The H + ICN reaction has three possible exit channels as given below:



Wittig and co-workers have studied the analogous H + ClCN reaction<sup>4</sup> and concluded that HCN + Cl was the predominant channel; the HCl + CN channel only accounted for about 15% of the reaction. Their ab initio calculations predicted that direct

attack on Cl leads to the HCl + CN channel, whereas sideways attack on C leads to HCN + Cl. Also attack on C could lead to HCl + CN, which would amount to H insertion between C and Cl. They found that direct attack on the N end is repulsive by over 50 kcal mol<sup>-1</sup>. Even though their calculations were in error by  $\approx 19 \text{ kcal mol}^{-1}$  on an absolute scale, these results give qualitative insight into analogous channels from reaction 1.

The H + ICN system differs from the H + ClCN system, because the HI + CN channel is endoergic and (1a) and (1b) are the only possible channels at 300 K. The exothermicity in reaction 1a is sufficient to populate several stretching ( $\nu_3 \leq 5$  or  $\nu_1 \leq 9$ ) and bending ( $\nu_2 \leq 23$ ) vibrational levels in HCN. Without any a priori knowledge of the system and considering the size of I relative to CN, attack on I might be anticipated. Often CN is considered as a pseudo-halogen and analogous behavior between ICN and IF might be expected. In H + IF reaction, in addition to direct attack on F, there is a second channel involving attack on the less electronegative I followed by migration to F.<sup>5</sup>

The HCN/HNC isomerization barrier is calculated to be 12 179 cm<sup>-1</sup> above the HCN minimum.<sup>6</sup> The exothermicity of reaction 1a, 16 625 cm<sup>-1</sup>, is well over this barrier. But quantum calculations<sup>7</sup> show that delocalization of HCN/HNC states does not occur for energies below 14 582 cm<sup>-1</sup>. These results and direct spectroscopic measurements of isolated states<sup>8</sup> show that even beyond this energy only states with several quanta of energy in the bending mode show any degree of delocalization. Also the density of states at this energy is still less than 1 state cm<sup>-1</sup>. On the basis of these findings, we believe that delocalization of HCN/HNC states is not important in our experiments; i.e., the HCN energy states can be described by the HCN spectroscopic constants.

## Experimental Procedure

The flowing afterglow IRCL apparatus in our laboratory has been described in detail before.<sup>9</sup> For the best conditions with Ar carrier gas, the pressure is 0.5 Torr and the reaction time is about 0.2 ms. The only change for these experiments is that the reagent, ICN, was introduced into the reactor by flowing Ar over the solid sample (Eastman Kodak Co). The H<sub>2</sub> concentration was  $1-5 \times 10^{13}$  molecules cm<sup>-3</sup> and the microwave discharge gives roughly 50% dissociation.<sup>9b</sup> The ICN concentration, estimated by weight loss of the ICN sample, was in the range  $(1-3) \times 10^{13}$  molecules cm<sup>-3</sup>. The IRCL was collected by using a BioRad FTS

(1) (a) Carrington, T.; Polanyi, J. C. *Int. Rev. Sci. Phys. Chem.* **1972**, *9*, 135. (b) Levine, R. D.; Bernstein, R. B. *Molecular Reaction Dynamics and Chemical Reactivity*; Oxford University Press: London, 1987. (c) Holmes, B. E.; Setser, D. W. In *Physical Chemistry of Fast Reactions*; Smith, I. W. M., Ed.; Plenum: New York, Vol. 2, p 83. (d) Agrawalla, B.; Setser, D. W. In *Gas Phase Chemiluminescence and Chemi-ionization*; Fontijn, A., Ed.; Elsevier: Amsterdam, 1985.

(2) Moehlmann, J. G.; Gleaves, J. T.; Hudgens, J. W.; McDonald, J. D. *J. Chem. Phys.* **1974**, *60*, 4790.

(3) Marciq, M. M.; Smith, M. A.; Simpson, C. J. S. M.; Ellison, G. B. *J. Chem. Phys.* **1981**, *74*, 6154.

(4) de Juan, J.; Callister, S.; Reiser, H.; Segal, G. A.; Wittig, C. *J. Chem. Phys.* **1988**, *89*, 1977.

(5) (a) Brandt, D.; Polanyi, J. C. *Chem. Phys.* **1980**, *45*, 65. (b) Tamagake, K.; Setser, D. W. *J. Phys. Chem.* **1979**, *83*, 1000.

(6) Murrell, J. N.; Carter, S.; Halonen, L. O. *J. Mol. Spectrosc.* **1982**, *93*, 307.

(7) Basic, Z.; Light, J. C. *J. Chem. Phys.* **1987**, *86*, 3065.

(8) (a) Yang, X.; Rogaski, C. A.; Woodtke, A. M. *J. Chem. Phys.* **1990**, *92*, 2111. (b) Lehmann, K. K.; Scherer, G. J.; Klemperer, W. *J. Chem. Phys.* **1982**, *77*, 2853.

(9) (a) Wategaonkar, S. J. Ph.D. Thesis, Kansas State University, 1988. (b) Wategaonkar, S. J.; Setser, D. W. *J. Chem. Phys.* **1989**, *90*, 251.

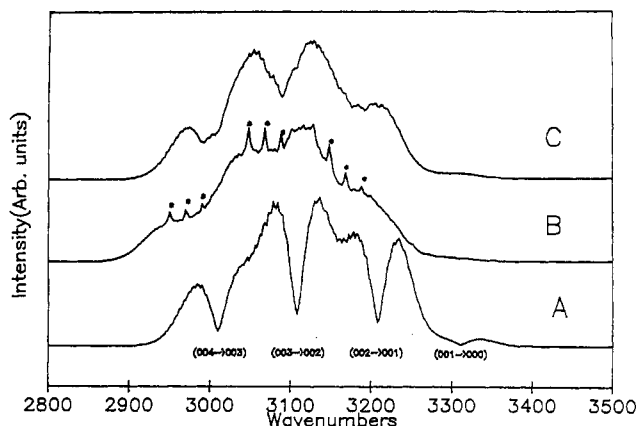


**Figure 1.** Simulated HCN emission spectra. (A)  $\Delta v_3 = 1$  from  $v_3 = 1-4$  without bending or CN stretch excitation.  $P_0$  is 5:40:40:15. (B)  $\Delta v_3 = 1$  spectra with 5, 4, 3, and 3 quanta in bending associated with  $v_3 = 1, 2, 3,$  and  $4$ . The bending distribution is inverted peaking in the middle; i.e., for  $v_3 = 1$ , the bending distribution is 1:2:3:3:2:1 for  $v_2 = 0-5$ . The  $P_0$  in  $v_3$  is the same as in A. \* denotes the Q branches observed when  $l > 0$ . (C)  $\Delta v_3 = 1$  spectra with 4, 3, 2, and 1 quanta in CN stretch (the distribution peaked in the middle as for  $v_2$  in B) associated with  $v_3 = 1, 2, 3,$  and  $4$ . The  $P_0$  for  $v_3$  is the same as in A.

60 FTIR with 2 or 4  $\text{cm}^{-1}$  resolution.

### Spectral Simulation

The HCN  $\Delta v_3 = 1$  emission spectrum consists of separate rotational lines corresponding to each vibrational-rotational level. Since the rotational constant  $B_0$  is about  $1.5 \text{ cm}^{-1}$ , the spacing between rotational lines is  $3 \text{ cm}^{-1}$ , whereas our resolution was only  $2 \text{ cm}^{-1}$ . This small  $B$  value leads to many rotational levels being populated at 300 K (the most probable  $J$  is 8). The excitation of  $v_1$  and  $v_2$  or higher levels of  $v_3$  leads to a shift in band centers for the  $\Delta v_3 = 1$  transition. These complications make simulation the only way to extract a vibrational distribution from the observed emission; the rotational distribution will be 300 K Boltzmann. Fortunately all the vibrational-rotational constants for HCN have been accurately determined,<sup>10</sup> making the simulation straightforward. The detailed spectroscopy associated with the  $v_2$  must be considered. For  $v_2 > 0$ , the vibrational angular momentum  $l$  is included in the term values and  $l$  can take values from 0 or 1 to  $v_2$ , in steps of 2, depending on whether  $v_2$  is even or odd.

$$E(v,l,J) = G(v,l) + F(v,l,J) \quad (2)$$

$$G(v,l) = \sum_i w_i \left( v_i + \frac{d_i}{2} \right) + \sum_i \sum_j x_{ij} \left( v_i + \frac{d_i}{2} \right) \left( v_j + \frac{d_j}{2} \right) + g_{22} l^2 + \sum_i \sum_j \sum_k y_{ijk} \left( v_i + \frac{d_i}{2} \right) \left( v_j + \frac{d_j}{2} \right) \left( v_k + \frac{d_k}{2} \right) + \sum_i y_{iii} \left( v_i + \frac{d_i}{2} \right)^2 \quad (3)$$

$$F(v,l,J) =$$

$$B_v(J+1)J - D_v(J(J+1) - l^2)^2 + H_v(J(J+1) - l^2)^3 \quad (4)$$

The fundamental transitions in  $v_3$ , such as  $0,0,n \rightarrow 0,0,(n-1)$  are  $\Sigma-\Sigma$  bands with P and R branches. For  $v_2 > 0$ , there are several possibilities such as  $\Sigma-\Sigma$ ,  $\Pi-\Pi$ ,  $\Delta-\Delta$ , etc., depending on whether  $l = 0, 1,$  or  $2$  respectively. For  $l > 0$  there are Q branches in addition to P and R branches.

The Einstein coefficients for rotationless transitions were taken from the theoretical calculations of Botschwina.<sup>11</sup> For  $\Delta v_3 = 1$ , these are 77.2, 135.6, 177.4, and  $205.4 \text{ s}^{-1}$  for  $v_3 = 1-4$ , respectively. The line strength factors for P, Q, and R branches are given by Hönl-London factors. (See Appendix in ref 10). The

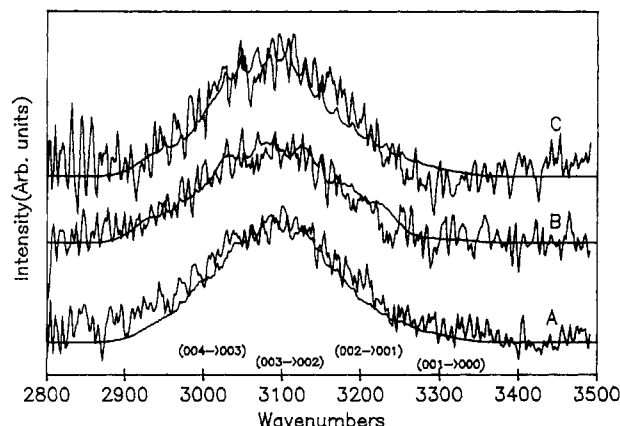


**Figure 2.** Experimental HCN emission spectra under different conditions. The Ar pressures and observation times for each spectrum were (A) 0.4 Torr, 0.30 ms; (B) 0.85 Torr, 0.25 ms; (C) 1.0 Torr, 0.32 ms. The product of Ar pressure and observation time varies from  $1.2 \times 10^{-4}$  to  $3.2 \times 10^{-4}$  Torr s.  $[\text{H}_2]$  was  $2 \times 10^{13} \text{ mol cm}^{-3}$ . The solid lines show simulated spectra. (A) Spectrum from just  $v_3 = 1$  with up to 17 quanta in bending, distribution peaking at  $v_2 = 8$ . (B) Spectrum from a  $v_3$  distribution of 5:35:45:15 with 3 quanta in  $v_2$  for each  $v_3$  level. The  $v_2$  distribution was uniform. (C) Spectrum from a  $v_3$  distribution of 30:45:20:5 with up to 8, 7, 5, and 3 quanta in  $v_2$  with an inverted distribution centered at the midlevel.

Einstein coefficients for transitions with  $v_2 > 0$  were assumed to be the same as those for transitions with  $v_2 = 0$  (i.e.,  $0,1,1 \rightarrow 0,1,0$  has the same Einstein coefficient as  $0,0,1 \rightarrow 0,0,0$ ). In our simulations  $l$ -type splitting was not considered because they cannot be resolved even for  $2 \text{ cm}^{-1}$  resolution.

Figure 1 shows some simulated spectra with and without  $v_2$  or  $v_1$  excitations, using  $4 \text{ cm}^{-1}$  Lorentzian line width for each rotational line. In principle, matching experimental and simulated spectra can give estimates of vibrational distribution in all three modes. But because of the strong overlap between several bands, the distribution obtained by simulation will not be unique. For example, the band centers for  $(0,0,3) \rightarrow (0,0,2)$  and  $(0,5,2) \rightarrow (0,5,1)$  are both at  $3108 \text{ cm}^{-1}$ , and for the other bending levels they lie between the  $(0,0,3)$  and the  $(0,0,2)$  bands. We must consider experimental trends based upon various operating conditions to choose one distribution over another, from a set that may fit a given experimental spectrum.

### Experimental Results

**a. Vibrational Distributions.** In order to determine the nascent vibrational spectrum several experiments were done with varying reaction conditions. We will argue that HCN( $v_3$ ) relaxation is arrested and that  $v_2$  relaxation is largely arrested for the lowest pressure and shortest reaction time. Figure 2 shows some HCN spectra obtained for 0.4–1.0 Torr and reaction times from 0.25 to 0.32 ms (the product of pressure and time varied from  $1.2 \times 10^{-4}$  to  $3.2 \times 10^{-4}$  Torr s); there is no evident change in the spectra. Smith and co-workers have studied the relaxation of HCN( $0,m,n$ ) by noble gases and several diatomic molecules.<sup>12</sup> Their rate constant of  $5.6 \times 10^{-15} \text{ cm}^3 \text{ s}^{-1}$  for Ar suggests 2–7% relaxation for (001) level for the conditions in Figure 2. The HCN( $0,0,1$ ) state is expected to relax through the  $(1,2,0)$  state. But unlike the HX molecules, relaxation rate constants for HCN<sup>13</sup> were found to decrease with increase in  $v_3$ , because the energy gap between  $(0,0,n)$  and  $(1,2,n-1)$  increases with increase in  $n$ . Our observed spectra are consistent with the higher  $v_3$  states having similar or smaller rate constants with Ar than  $5.6 \times 10^{-15} \text{ cm}^3 \text{ s}^{-1}$ . For these and other conditions, varying the  $\text{H}_2$  or ICN concentration within the range used to collect data did not cause any appreciable relaxation. Figure 3 shows that changing  $[\text{H}_2]$  at  $P\Delta t = 4.8 \times 10^{-4}$  Torr s caused no change in the observed spectra.

(10) Smith, A. M.; Coy, S. L.; Klemperer, W.; Lehmann, K. K. *J. Mol. Spectrosc.* **1989**, *134*, 134.

(11) Botschwina, P. *Chem. Phys.* **1983**, *81*, 73.

(12) Cannon, B. D.; Smith, I. W. M. *Chem. Phys.* **1984**, *83*, 429.

(13) Hastings, P. W.; Osborn, M. K.; Sadowski, C. M.; Smith, I. W. M. *J. Chem. Phys.* **1983**, *78*, 3893.

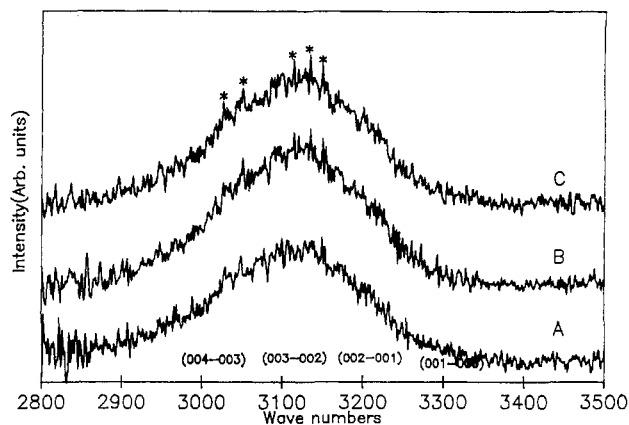


**Figure 3.** Experimental HCN spectrum for 0.4 ms reaction time and 1.2 Torr of Ar, for various  $[H]$  (in  $10^{13}$  molecules  $\text{cm}^{-3}$ ). (A) 2.4; (B) 3.7; (C) 4.8. The \* denotes the expected region for Q-branch transitions, which are observed. These experiments showed that changing  $[H_2]$  and ICN did not cause relaxation.

The wavelength range for the emission band and the absence of any minima in the spectra indicate high  $\nu_3$  excitation up to  $\nu_3 = 4$ , but also concomitant  $\nu_2$  and/or  $\nu_1$  excitation. The relaxation rate of CN stretch would be expected to be similar to that of CH stretch. But the bending mode could relax faster and according to Smith and co-workers the rate constant for the  $(0,1,1) \rightarrow (0,0,1)$  process is  $1.2 \times 10^{-13}$   $\text{cm}^3 \text{s}^{-1}$ . This corresponds to 30% relaxation even under our best conditions. But the data in Figure 2 do not suggest this high degree of relaxation. Marciq et al.<sup>3</sup> have also reported estimates of relaxation rate constants for the bending levels  $(0,n,0)$ . For Ar they give an upper limit of  $3.1 \times 10^{-14}$   $\text{cm}^3 \text{s}^{-1}$ , which corresponds to 10% relaxation for our best condition. Our experiments favor this lower rate constant. Generally  $\nu$ - $T$  rates increase with higher levels for diatomic molecules, but possibly this is not the case for the bending mode of HCN.

Some experiments were carried out at longer reaction time, 0.5 ms, with Ar pressure ranging from 0.6 to 2.0 Torr in order to force some vibrational relaxation; see Figure 4. According to ref 12, the relaxation of the HCN(0,0, $n$ ) by Ar should be only from 5 to 18% for these conditions. Thus we believe that relaxation of the bending mode must be largely responsible for the shift of the emission observed in Figure 4, suggesting bending mode excitation rather than CN stretch excitation to be the cause of the observed broadening. We have two other arguments against  $\nu_1$  excitation being the dominant source for the broadening. First, some of the Q branches of the  $(0,m,n) \rightarrow (0,m,n-1)$  transitions can be observed in the spectrum, giving positive evidence for the bending mode excitation (see Figure 3). Secondly, at least 3 or 4 quanta of CN stretch with 3 or 4 quanta in CH stretch are needed to account for the observed broadening, but the available energy from (1a) is insufficient for such high vibrational excitations. Hence we favor combined  $\nu_3$  and  $\nu_2$  excitation to explain the nascent spectrum. At this point we would like to point out that under slightly relaxed conditions we could see the Q branches of transitions such as  $(1,3,2) \rightarrow (1,3,1)$ , where all three modes have been excited. But, these levels could be formed by relaxation of higher levels as discussed earlier.

The vibrational distributions of  $\nu_2$  and  $\nu_3$  were varied in a systematic fashion to simulate the nascent emission spectrum. Due to the overlap in bands, the data can be fitted with different distributions in  $\nu_2$  and  $\nu_3$ ; see Figure 2. We first assigned an upper limit to  $\nu_3$  excitation by using the minimum excitation in  $\nu_2$  that is required to fit the observed spectrum. The best fit corresponds to an initial  $\nu_3$  population as  $P_1:P_2:P_3:P_4 = 5:35:45:15$  with three quanta in  $\nu_2$  with equal population, for each  $\nu_3$  level. This corresponds to an  $\langle f_v \rangle$  of 0.58 with  $\langle f_v \rangle$  from just  $\nu_3$  excitation of 0.52. On the other extreme we could fit the experimental spectrum with all the population in  $\nu_3 = 1$  and an inverted distribution in  $\nu_2$  peaking at  $\nu_2 = 8$  and extending to  $\nu_2 = 17$ . Only  $l$  values 0-2 were considered in the simulation to reduce the number of rotational lines. This distribution again corresponds to an  $\langle f_v \rangle$  of

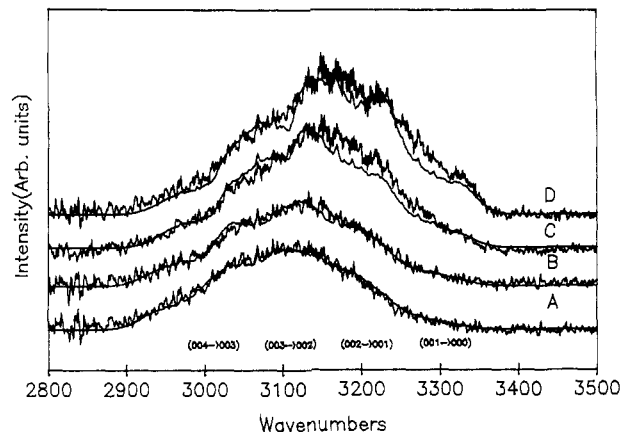


**Figure 4.** Effect of increasing Ar pressure at constant observation time (0.5 ms) and  $[H]$  ( $5 \times 10^{13}$ ) (A) 0.6 Torr; (B) 1.0 Torr; (C) 1.5 Torr; (D) 2.0 Torr. The simulated spectra have a fixed  $\nu_3$  distribution of  $P_1-P_4 = 30:45:20:5$ . The bending distribution associated with each  $\nu_3$  level changes for each spectrum. (A)  $\nu_2(\text{max}) = 8, 7, 5,$  and  $3$ ; the most probable  $\nu_2$  is  $5, 4, 3,$  and  $2$ . (B)  $\nu_2(\text{max}) = 7, 6, 4,$  and  $3$ ; the most probable  $\nu_2$  is  $4, 3, 2,$  and  $1$ . (C)  $\nu_2(\text{max}) = 6, 5, 4,$  and  $3$ . The most probable  $\nu_2$  is  $2, 2, 1,$  and  $0$ . (D)  $\nu_2(\text{max}) = 5, 4, 3,$  and  $2$ ; the most probable  $\nu_2$  is  $1, 1, 1,$  and  $0$ .

0.57, but the  $\langle f_v \rangle$  from  $\nu_3$  alone is now 0.20 only. These two examples show that there could be other distributions with intermediate  $\nu_2$  and  $\nu_3$  excitations but the  $\langle f_v \rangle$  (HCN) will be more or less the same irrespective of the assigned distribution. In order to differentiate between these distributions we fitted the spectra in Figure 4. With an initial  $\nu_3$  distribution of  $P_1-P_4 = 30:45:20:5$  with up to 8, 7, 5, and 3 quanta in  $\nu_2$  corresponding to  $\nu_3 = 1-4$ , respectively, we can fit the nascent spectrum. By allowing only bending mode relaxation we can fit all the spectra in Figure 4. Hence we favor the intermediate distribution just quoted for  $\nu_3$ . The  $\langle f_v \rangle$  values that have been quoted do not include any bending excitation that might be associated with  $\nu_3 = 0$ . Thus, these values are probably lower estimates to true  $\langle f_v \rangle$ .

Besides HCN emission we also observed HNC(0,0,1)  $\rightarrow$  (0,0,0) emission. The signal was about 1% of the HCN emission signal. As the Einstein coefficient for HNC has been predicted to be 5 times higher than HCN,<sup>14</sup> clearly HNC formation is a minor channel. The isomerization barrier of about 14 600  $\text{cm}^{-1}$  is less than the exothermicity of the reaction, but if HNC is formed by isomerization high vibrational excitation should be observed in HNC; i.e., only HCN states with energy greater than 14 600  $\text{cm}^{-1}$  could isomerize to give HNC, which corresponds to an  $\langle E_v \rangle$  of about 10 000  $\text{cm}^{-1}$  in HNC. But since only  $(0,0,1) \rightarrow (0,0,0)$  emission was observed, we believe isomerization is not the mechanism for HNC formation.

**b. HCN Formation Rate Constant.** In order to measure the rate constant for HCN formation, the overall intensities from H + ICN and Cl<sub>2</sub> were compared for the same  $[H_2]$  and reaction time. The observed intensities were corrected for instrumental response function and the Einstein coefficients before comparison. The observed HCl( $\nu$ ) distribution was  $P_{1-4} = 12:38:40:10$  as expected.<sup>9</sup> Under our conditions the differential rate law holds and so the ratio of HCl and HCN products gives the ratio of the formation rate constants.

$$\frac{\text{HCN}(\nu_3 \geq 1)}{[\text{HCl}(\nu \geq 1)]} = \frac{k_{\text{HCl}}[H][\text{Cl}_2]}{k_{\text{HCN}}[H][\text{ICN}]} \quad (5)$$

The rate constant for the HCN formation,  $(2.0 \pm 0.4) \times 10^{-12}$   $\text{cm}^3 \text{s}^{-1}$ , is only about 1/10th of the H + Cl<sub>2</sub> reaction.<sup>15</sup> The uncertainties in the measurements include the nascent  $\nu_3 = 0$  population, the HCN Einstein coefficients, and flow rate measurements. The smaller rate constant is partly compensated by the larger Einstein coefficients (74  $\text{s}^{-1}$  for HCN vs 40  $\text{s}^{-1}$  for HCl

(14) Rogers, J. D.; Hillman, J. J. *J. Chem. Phys.* **1982**, *77*, 3615.

(15) Bemand, P. B.; Clyne, M. A. A. *J. Chem. Soc., Faraday Trans. 2* **1977**, *73*, 394.

for  $\nu = 1 \rightarrow 0$ ) making it possible to obtain the IRCL spectrum of HCN.

### Discussion and Conclusions

The H + ICN reaction primarily leads to HCN(0,  $m$ ,  $n$ ) + I, but there is a minor channel producing HNC + I. The HNC is directly formed from the reaction 1b, rather than by isomerization. The rate constant for HCN formation is  $(2.0 \pm 0.4) \times 10^{-12} \text{ cm}^3 \text{ s}^{-1}$  at room temperature. The HCN( $\nu_1, \nu_2, \nu_3$ ) distribution offers direct evidence into the dynamics of the H + ICN reaction. The highly inverted distribution is in strong contrast with the HX distributions obtained in unimolecular elimination or displacement reactions,<sup>14,16</sup> which implies that the reaction does not proceed through a bound HICN intermediate. At first glance this may seem surprising because the triply bonded CN offers a position where the H could add. In the H + ClCN case the calculations found HClCN to be bound by only 6 kcal mol<sup>-1</sup>. We believe that HICN would be bound by even less than 6 kcal mol<sup>-1</sup>, or probably it is not bound at all. Comparing the HCN distribution from H + ICN, BrCN, and ClCN would be interesting. If there is a systematic change in the stability of the intermediates, the dynamics of these reactions would be affected and lead to different HCN distributions. Our preliminary results from H + BrCN seem to suggest a lower  $\langle f_\nu(\text{HCN}) \rangle$ , indicating a greater role for a bound intermediate.

The partitioning between  $\nu_3$  and  $\nu_2$  could offer additional insight into the dynamics. Unfortunately, our interpretations are strongly affected by our assumption that  $\nu_2$  relaxation should be faster than  $\nu_3$ . Nevertheless, substantial bending excitation is required to fit the spectra. It is likely that H either directly attacks the C or it adds to the I end and then migrates to C to form HCN + I. In both cases H will more or less add to the C perpendicularly and transform to the linear HCN molecule, as HCN and I separate. This can clearly produce bending mode excitation as has

been observed. Since the CN probably moves as one unit relative to the light H atom, significant excitation of the CN stretch is very unlikely.

The vibrational distribution and  $\langle f_\nu \rangle$  observed in migratory reactions and direct displacement reactions from H + BrF and IF are worth comparing to the present data. The  $\langle f_\nu \rangle$  for all these reactions are about the same, ranging from 0.5 to 0.7, but the observed distribution and rotational excitation differ significantly for the two microscopic pathways. The migratory channel results in broader rotational distribution, whereas the displacement channel has less rotational excitation. With HCN, under our experimental conditions it is not possible to infer anything about rotational distribution, but migration may affect the bending mode excitation. As we learn more about HCN( $\nu_1, \nu_2, \nu_3$ ) state to state relaxation processes,<sup>17</sup> these interpretations should be possible.

The IRCL of HCN offers considerable opportunity to study the dynamics of reactions yielding HCN as a product. With higher resolution experiments, it will be possible to obtain better population assignments. The  $\nu_3$  emission not only provides information similar to that from HX emission for inferring details about the dynamics but also reveals new information from excitation in the bending mode. For example, the reaction of H atom with *tert*-butyronitrile<sup>18</sup> gives only (0,0,1)  $\rightarrow$  (0,0,0) emission without any bending excitation. In this case the H may approach the C end and displace butyl to form HCN via a bound intermediate. Another possibility would be to study the HCN from abstraction of H from a series of molecules by CN. The IRCL of HCN should develop into an important area of chemical reaction dynamics to complement the currently active SEP studies.<sup>8a</sup>

*Acknowledgment.* This work was supported by the National Science Foundation, Grant CHE 8822060. We thank Dr. Glenn Lo for providing the XYCALC program which was used to convolute the simulated spectra.

(16) Arunan, E.; Wategaonkar, S. J.; Setser, D. W. *J. Phys. Chem.* 1991, 95, 1539.

(17) Smith, I. W. M.; Warr, J. F. *J. Chem. Soc., Faraday. Trans.* 1991, 87, 205.

(18) Wategaonkar, S. J.; Setser, D. W. Unpublished results.

## Observation of Magic Numbers within Ar<sub>n</sub>H<sub>2</sub>O<sup>+</sup> Heteroclusters

Gopal Vaidyanathan, M. Todd Coolbaugh, William R. Peifer, and James F. Garvey\*

Department of Chemistry, Acheson Hall, State University of New York at Buffalo, Buffalo, New York 14214  
(Received: March 12, 1991)

We present in this communication the observation of magic numbers for the heterocluster ion Ar<sub>n</sub>H<sub>2</sub>O<sup>+</sup> for  $n = 3, 9$ , and 15 which we attribute to the stability of the cluster ion. On comparison with the calculations of Bohmer and Peyerimhoff for Ar<sub>n</sub>Xe<sup>+</sup>, we feel this data suggests that, in the case of Ar<sub>n</sub>H<sub>2</sub>O<sup>+</sup>, the water cation sits at the center of the argon cluster, representing the first example of an oxygen-containing molecule exhibiting such behavior. However, while Bohmer and Peyerimhoff predict a magic number for Ar<sub>12</sub>Xe<sup>+</sup>, we do not observe one for Ar<sub>12</sub>H<sub>2</sub>O<sup>+</sup>. We postulate that this difference may be due to the water cation distorting the structure of the solvating argons.

The study of van der Waals clusters has aroused a great deal of interest in recent years<sup>1-5</sup> due to the unique position that clusters hold between the gas and condensed phases of matter.<sup>6,7</sup> Theoretical and experimental studies of these isolated clusters have provided considerable insights<sup>8,9</sup> into changes in their physical and

chemical properties as a function of cluster size.

Mass spectrometric studies of gas-phase clusters, in particular, have proved extremely useful through the observation of magic numbers (i.e., anomalous enhancements of cluster ion signal for a specific cluster size). The observation of a magic number typically indicates a particularly stable cluster ion stoichiometry, from which the cluster ion geometry can often be inferred. In the case of molecular systems this stability is typically attributed to a stable, closed solvent shell, hydrogen bonded directly to a central cation.<sup>10-14</sup> In recent years the study of magic numbers

(1) Levy, D. H. *Adv. Chem. Phys.* 1981, 47, 323.

(2) Ng, C. Y. *Adv. Chem. Phys.* 1983, 52, 152.

(3) Märk, T. D.; Castleman Jr., A. W. *Adv. At. Mol. Phys.* 1985, 20, 65.

(4) Jortner, J. *Ber. Bunsen-Ges. Phys. Chem.* 1984, 88, 188.

(5) *Atomic and Molecular Beam Methods*; Scoles, G., Ed.; Oxford University Press: New York, 1988.

(6) *Physics and Chemistry of Small Clusters*; NATO ASI Series B; Jena, P., Rao, B. K., Khanna, S. N., Eds.; Plenum: New York, 1987; p 158.

(7) Castleman, Jr., A. W.; Märk, T. D. *Gaseous Ion Chemistry and Mass Spectrometry*; Futrell, J. H., Ed.; Wiley Interscience: New York, 1981.

(8) Hagena, O. F.; Obert, W. *J. Chem. Phys.* 1972, 56, 1793.

(9) S. D. Stein Memorial Issue. *J. Phys. Chem.* 1987, 91.

(10) Stace, A. J.; Moore, C. J. *J. Phys. Chem.* 1982, 86, 3681.